Fermi National Accelerator Laboratory

FERMILAB-Pub-97/286-E
CDF

Measurement of the $t\bar{t}$ Production Cross Section in $p\bar{p}$ Collisions at $\sqrt{s}$ = 1.8 TeV

F. Abe et al.
The CDF Collaboration

Fermi National Accelerator Laboratory
P.O. Box 500, Batavia, Illinois 60510

October 1997

Submitted to *Physical Review Letters*

Operated by Universities Research Association Inc. under Contract No. DE-AC02-76CH03000 with the United States Department of Energy

Fermilab-Pub 97/286-E

Measurement of the $t\bar{t}$ Production Cross Section in $p\bar{p}$ Collisions at $\sqrt{s} = 1.8$ TeV

F. Abe,[17] H. Akimoto,[39] A. Akopian,[31] M. G. Albrow,[7] A. Amadon,[5] S. R. Amendolia,[27] D. Amidei,[20] J. Antos,[33] S. Aota,[37] T. Arisawa,[39] T. Asakawa,[37] W. Ashmanskas,[18] M. Atac,[7] P. Azzi-Bacchetta,[25] N. Bacchetta,[25] S. Bagdasarov,[31] M. W. Bailey,[22] P. de Barbaro,[30] A. Barbaro-Galtieri,[18] V. E. Barnes,[29] B. A. Barnett,[15] M. Barone,[9] G. Bauer,[19] T. Baumann,[11] F. Bedeschi,[27] S. Behrends,[3] S. Belforte,[27] G. Bellettini,[27] J. Bellinger,[40] D. Benjamin,[35] J. Bensinger,[3] A. Beretvas,[7] J. P. Berge,[7] J. Berryhill,[5] S. Bertolucci,[9] S. Bettelli,[27] B. Bevensee,[26] A. Bhatti,[31] K. Biery,[7] C. Bigongiari,[27] M. Binkley,[7] D. Bisello,[25] R. E. Blair,[1] C. Blocker,[3] S. Blusk,[30] A. Bodek,[30] W. Bokhari,[26] G. Bolla,[29] Y. Bonushkin,[4] D. Bortoletto,[29] J. Boudreau,[28] L. Breccia,[2] C. Bromberg,[21] N. Bruner,[22] R. Brunetti,[2] E. Buckley-Geer,[7] H. S. Budd,[30] K. Burkett,[20] G. Busetto,[25] A. Byon-Wagner,[7] K. L. Byrum,[1] M. Campbell,[20] A. Caner,[27] W. Carithers,[18] D. Carlsmith,[40] J. Cassada,[30] A. Castro,[25] D. Cauz,[36] A. Cerri,[27] P. S. Chang,[33] P. T. Chang,[33] H. Y. Chao,[33] J. Chapman,[20] M. -T. Cheng,[33] M. Chertok,[34] G. Chiarelli,[27] C. N. Chiou,[33] L. Christofek,[13] M. L. Chu,[33] S. Cihangir,[7] A. G. Clark,[10] M. Cobal,[27] E. Cocca,[27] M. Contreras,[5] J. Conway,[32] J. Cooper,[7] M. Cordelli,[9] D. Costanzo,[27] C. Couyoumtzelis,[10] D. Cronin-Hennessy,[6] R. Culbertson,[5] D. Dagenhart,[38] T. Daniels,[19] F. DeJongh,[7] S. Dell'Agnello,[9] M. Dell'Orso,[27] R. Demina,[7] L. Demortier,[31] M. Deninno,[2] P. F. Derwent,[7] T. Devlin,[32] J. R. Dittmann,[6] S. Donati,[27] J. Done,[34] T. Dorigo,[25] N. Eddy,[20] K. Einsweiler,[18] J. E. Elias,[7] R. Ely,[18] E. Engels, Jr.,[28] D. Errede,[13] S. Errede,[13] Q. Fan,[30] R. G. Feild,[41] Z. Feng,[15] C. Ferretti,[27] I. Fiori,[2] B. Flaugher,[7] G. W. Foster,[7] J. Freeman,[7] J. Friedman,[19] H. Frisch,[5] Y. Fukui,[17] S. Galeotti,[27] M. Gallinaro,[26] O. Ganel,[35] M. Garcia-Sciveres,[18] A. F. Garfinkel,[29] C. Gay,[41] S. Geer,[7] D. W. Gerdes,[15]

P. Giannetti,[27] N. Giokaris,[31] G. Giusti,[27] M. Gold,[22] A. T. Goshaw,[6] Y. Gotra,[25]
K. Goulianos,[31] H. Grassmann,[36] L. Groer,[32] C. Grosso-Pilcher,[5] G. Guillian,[20]
J. Guimaraes da Costa,[15] R. S. Guo,[33] C. Haber,[18] E. Hafen,[19] S. R. Hahn,[7] R. Hamilton,[11]
T. Handa,[12] R. Handler,[40] F. Happacher,[9] K. Hara,[37] A. D. Hardman,[29] R. M. Harris,[7]
F. Hartmann,[16] J. Hauser,[4] E. Hayashi,[37] J. Heinrich,[26] W. Hao,[35] B. Hinrichsen,[14]
K. D. Hoffman,[29] M. Hohlmann,[5] C. Holck,[26] R. Hollebeek,[26] L. Holloway,[13] Z. Huang,[20]
B. T. Huffman,[28] R. Hughes,[23] J. Huston,[21] J. Huth,[11] H. Ikeda,[37] M. Incagli,[27]
J. Incandela,[7] G. Introzzi,[27] J. Iwai,[39] Y. Iwata,[12] E. James,[20] H. Jensen,[7] U. Joshi,[7]
E. Kajfasz,[25] H. Kambara,[10] T. Kamon,[34] T. Kaneko,[37] K. Karr,[38] H. Kasha,[41] Y. Kato,[24]
T. A. Keaffaber,[29] K. Kelley,[19] R. D. Kennedy,[7] R. Kephart,[7] D. Kestenbaum,[11]
D. Khazins,[6] T. Kikuchi,[37] B. J. Kim,[27] H. S. Kim,[14] S. H. Kim,[37] Y. K. Kim,[18] L. Kirsch,[3]
S. Klimenko,[8] D. Knoblauch,[16] P. Koehn,[23] A. Köngeter,[16] K. Kondo,[37] J. Konigsberg,[8]
K. Kordas,[14] A. Korytov,[8] E. Kovacs,[1] W. Kowald,[6] J. Kroll,[26] M. Kruse,[30]
S. E. Kuhlmann,[1] E. Kuns,[32] K. Kurino,[12] T. Kuwabara,[37] A. T. Laasanen,[29] I. Nakano,[12]
S. Lami,[27] S. Lammel,[7] J. I. Lamoureux,[3] M. Lancaster,[18] M. Lanzoni,[27] G. Latino,[27]
T. LeCompte,[1] S. Leone,[27] J. D. Lewis,[7] P. Limon,[7] M. Lindgren,[4] T. M. Liss,[13] J. B. Liu,[30]
Y. C. Liu,[33] N. Lockyer,[26] O. Long,[26] C. Loomis,[32] M. Loreti,[25] D. Lucchesi,[27] P. Lukens,[7]
S. Lusin,[40] J. Lys,[18] K. Maeshima,[7] P. Maksimovic,[19] M. Mangano,[27] M. Mariotti,[25]
J. P. Marriner,[7] A. Martin,[41] J. A. J. Matthews,[22] P. Mazzanti,[2] P. McIntyre,[34] P. Melese,[31]
M. Menguzzato,[25] A. Menzione,[27] E. Meschi,[27] S. Metzler,[26] C. Miao,[20] T. Miao,[7]
G. Michail,[11] R. Miller,[21] H. Minato,[37] S. Miscetti,[9] M. Mishina,[17] S. Miyashita,[37]
N. Moggi,[27] E. Moore,[22] Y. Morita,[17] A. Mukherjee,[7] T. Muller,[16] P. Murat,[27] S. Murgia,[21]
H. Nakada,[37] I. Nakano,[12] C. Nelson,[7] D. Neuberger,[16] C. Newman-Holmes,[7]
C.-Y. P. Ngan,[19] L. Nodulman,[1] S. H. Oh,[6] T. Ohmoto,[12] T. Ohsugi,[12] R. Oishi,[37]
M. Okabe,[37] T. Okusawa,[24] J. Olsen,[40] C. Pagliarone,[27] R. Paoletti,[27] V. Papadimitriou,[35]
S. P. Pappas,[41] N. Parashar,[27] A. Parri,[9] J. Patrick,[7] G. Pauletta,[36] M. Paulini,[18]
A. Perazzo,[27] L. Pescara,[25] M. D. Peters,[18] T. J. Phillips,[6] G. Piacentino,[27] M. Pillai,[30]
K. T. Pitts,[7] R. Plunkett,[7] L. Pondrom,[40] J. Proudfoot,[1] G. Punzi,[27] K. Ragan,[14]

D. Reher,[18] M. Reischl,[16] A. Ribon,[25] F. Rimondi,[2] L. Ristori,[27] W. J. Robertson,[6] T. Rodrigo,[27] S. Rolli,[38] L. Rosenson,[19] R. Roser,[13] T. Saab,[14] W. K. Sakumoto,[30] D. Saltzberg,[4] A. Sansoni,[9] L. Santi,[36] H. Sato,[37] P. Schlabach,[7] E. E. Schmidt,[7] M. P. Schmidt,[41] A. Scott,[4] A. Scribano,[27] S. Segler,[7] S. Seidel,[22] Y. Seiya,[37] F. Semeria,[2] T. Shah,[19] M. D. Shapiro,[18] N. M. Shaw,[29] P. F. Shepard,[28] T. Shibayama,[37] M. Shimojima,[37] M. Shochet,[5] J. Siegrist,[18] A. Sill,[35] P. Sinervo,[14] P. Singh,[13] K. Sliwa,[38] C. Smith,[15] F. D. Snider,[15] J. Spalding,[7] T. Speer,[10] P. Sphicas,[19] F. Spinella,[27] L. Spiegel,[7] L. Stanco,[25] J. Steele,[40] A. Stefanini,[27] R. Ströhmer,[7a] J. Strologas,[13] F. Strumia, [10] D. Stuart,[7] K. Sumorok,[19] J. Suzuki,[37] T. Suzuki,[37] T. Takahashi,[24] T. Takano,[24] R. Takashima,[12] K. Takikawa,[37] M. Tanaka,[37] B. Tannenbaum,[22] F. Tartarelli,[27] W. Taylor,[14] M. Tecchio,[20] P. K. Teng,[33] Y. Teramoto,[24] K. Terashi,[37] S. Tether,[19] D. Theriot,[7] T. L. Thomas,[22] R. Thurman-Keup,[1] M. Timko,[38] P. Tipton,[30] A. Titov,[31] S. Tkaczyk,[7] D. Toback,[5] K. Tollefson,[19] A. Tollestrup,[7] H. Toyoda,[24] W. Trischuk,[14] J. F. de Troconiz,[11] S. Truitt,[20] J. Tseng,[19] N. Turini,[27] T. Uchida,[37] F. Ukegawa,[26] S. C. van den Brink,[28] S. Vejcik, III,[20] G. Velev,[27] R. Vidal,[7] R. Vilar,[7a] D. Vucinic,[19] R. G. Wagner,[1] R. L. Wagner,[7] J. Wahl,[5] N. B. Wallace,[27] A. M. Walsh,[32] C. Wang,[6] C. H. Wang,[33] M. J. Wang,[33] A. Warburton,[14] T. Watanabe,[37] T. Watts,[32] R. Webb,[34] C. Wei,[6] H. Wenzel,[16] W. C. Wester, III,[7] A. B. Wicklund,[1] E. Wicklund,[7] R. Wilkinson,[26] H. H. Williams,[26] P. Wilson,[5] B. L. Winer,[23] D. Winn,[20] D. Wolinski,[20] J. Wolinski,[21] S. Worm,[22] X. Wu,[10] J. Wyss,[27] A. Yagil,[7] W. Yao,[18] K. Yasuoka,[37] G. P. Yeh,[7] P. Yeh,[33] J. Yoh,[7] C. Yosef,[21] T. Yoshida,[24] I. Yu,[7] A. Zanetti,[36] F. Zetti,[27] and S. Zucchelli[2]

(CDF Collaboration)

[1] *Argonne National Laboratory, Argonne, Illinois 60439*

[2] *Istituto Nazionale di Fisica Nucleare, University of Bologna, I-40127 Bologna, Italy*

[3] *Brandeis University, Waltham, Massachusetts 02254*

[4] *University of California at Los Angeles, Los Angeles, California 90024*

[5] *University of Chicago, Chicago, Illinois 60637*

[6] *Duke University, Durham, North Carolina 27708*

[7] *Fermi National Accelerator Laboratory, Batavia, Illinois 60510*

[8] *University of Florida, Gainesville, FL 32611*

[9] *Laboratori Nazionali di Frascati, Istituto Nazionale di Fisica Nucleare, I-00044 Frascati, Italy*

[10] *University of Geneva, CH-1211 Geneva 4, Switzerland*

[11] *Harvard University, Cambridge, Massachusetts 02138*

[12] *Hiroshima University, Higashi-Hiroshima 724, Japan*

[13] *University of Illinois, Urbana, Illinois 61801*

[14] *Institute of Particle Physics, McGill University, Montreal H3A 2T8, and University of Toronto, Toronto M5S 1A7, Canada*

[15] *The Johns Hopkins University, Baltimore, Maryland 21218*

[16] *Institut für Experimentelle Kernphysik, Universität Karlsruhe, 76128 Karlsruhe, Germany*

[17] *National Laboratory for High Energy Physics (KEK), Tsukuba, Ibaraki 305, Japan*

[18] *Ernest Orlando Lawrence Berkeley National Laboratory, Berkeley, California 94720*

[19] *Massachusetts Institute of Technology, Cambridge, Massachusetts 02139*

[20] *University of Michigan, Ann Arbor, Michigan 48109*

[21] *Michigan State University, East Lansing, Michigan 48824*

[22] *University of New Mexico, Albuquerque, New Mexico 87131*

[23] *The Ohio State University, Columbus, OH 43210*

[24] *Osaka City University, Osaka 588, Japan*

[25] *Universita di Padova, Istituto Nazionale di Fisica Nucleare, Sezione di Padova, I-36132 Padova, Italy*

[26] *University of Pennsylvania, Philadelphia, Pennsylvania 19104*

[27] *Istituto Nazionale di Fisica Nucleare, University and Scuola Normale Superiore of Pisa, I-56100 Pisa, Italy*

[28] *University of Pittsburgh, Pittsburgh, Pennsylvania 15260*

[29] *Purdue University, West Lafayette, Indiana 47907*

[30] *University of Rochester, Rochester, New York 14627*

[31] *Rockefeller University, New York, New York 10021*

[32] *Rutgers University, Piscataway, New Jersey 08855*

[33] *Academia Sinica, Taipei, Taiwan 11530, Republic of China*

[34] *Texas A&M University, College Station, Texas 77843*

[35] *Texas Tech University, Lubbock, Texas 79409*

[36] *Istituto Nazionale di Fisica Nucleare, University of Trieste/ Udine, Italy*

[37] *University of Tsukuba, Tsukuba, Ibaraki 315, Japan*

[38] *Tufts University, Medford, Massachusetts 02155*

[39] *Waseda University, Tokyo 169, Japan*

[40] *University of Wisconsin, Madison, Wisconsin 53706*

[41] *Yale University, New Haven, Connecticut 06520*

(October 9, 1997)

Abstract

We present a measurement of the $t\bar{t}$ production cross section in $p\bar{p}$ collisions at $\sqrt{s} = 1.8$ TeV using an integrated luminosity of 109 pb^{-1} collected with the Collider Detector at Fermilab. The measurement uses $t\bar{t}$ decays into final states which contain one or two high transverse momentum leptons and multiple jets, and final states which contain only jets. Using acceptances appropriate for a top quark mass of 175 GeV/c^2, we find $\sigma_{t\bar{t}} = 7.6^{+1.8}_{-1.5}$ pb.

14.65 Ha, 13.85 Ni, 13.85 Qk

The measurement of the $p\bar{p} \rightarrow t\bar{t}\ X$ production cross section presents a test of both the production and decay mechanisms of the standard model. Recent calculations [1] based on Quantum Chromodynamics (QCD) have led to predictions for the cross section with a theoretical uncertainty of less than 15%. A measurement that is significantly different from the predicted value can signal either non-standard model production, for instance the decay of a heavy resonance into $t\bar{t}$ pairs, or a non-standard model decay mechanism such as the decay into supersymmetric particles [2]. In the latter case it is of particular interest to measure the cross section into different final states, because an unexpected decay mode of the top quark will modify the expected branching fractions. The $t\bar{t}$ production cross section has been measured before by both the Collider Detector at Fermilab (CDF) and D0 collaborations [3–5].

The standard model predicts that the top quark will decay nearly 100% of the time to Wb. The W boson can then decay to either a pair of quarks, or a lepton neutrino ($\ell\nu$) pair. We categorize the decays of $t\bar{t}$ pairs by the decays of the two W bosons as either lepton+jets, dilepton, or all-hadronic. The dilepton and all-hadronic analyses are described elsewhere [6,7]. We now have nearly twice as much data as reported in [4]. With improved measurements of acceptances and backgrounds, and by combining all the decay modes, we measure the cross section with better than twice the precision of our previous measurement.

The data presented here represent the entire data set accumulated between 1992 and 1995 with the CDF detector, and corresponds to an integrated luminosity of 109 ± 7 pb^{-1} (19 pb^{-1} from the 1992-93 run and 90 pb^{-1} from the 1994-95 run) [8].

The CDF detector consists of a magnetic spectrometer surrounded by calorimeters and muon chambers. A four-layer silicon vertex detector (SVX), located immediately outside the beam pipe, provides precise track reconstruction in the plane transverse to the beam and is used to identify secondary vertices from b and c quark decays. A detailed description of the detector can be found elsewhere [3,9].

The electron, muon, and multi-jet events used in this analysis were selected by a three-level trigger. Lepton samples were acquired with inclusive electron and muon triggers requiring P_T(lepton)$>$ 18 GeV/c. A missing transverse energy [3], $\not\!\!E_T$, trigger was also used in order to recover events lost due to small inefficiencies in the inclusive lepton triggers.

Decays of $t\bar{t}$ pairs into lepton+jets are characterized by a single high-P_T lepton, missing transverse energy from the $W \to \ell\nu$ decay, plus four jets, two from the hadronically decaying W boson and two from the b quarks from the top decays. Jets are defined using a cone algorithm with $\Delta R = \sqrt{\Delta\phi^2 + \Delta\eta^2}$=0.4, where η is the pseudo-rapidity. Jets are counted in this analysis if $|\ \eta\ | < 2.0$. The number of observed jets may decrease due to detector effects or jet overlap, or increase as a result of multiple interactions or the presence of gluon radiation. In the lepton+jets channel, events with three or more jets with measured E_T >15 GeV define the $t\bar{t}$ signal region.

The data sample for the lepton+jets analysis is a subset of a sample of high-P_T inclusive lepton events that contain either an isolated electron with $E_T > 20$ GeV or an isolated muon with $P_T > 20$ GeV/c in the central region ($|\ \eta\ |$<1.0). Events that contain a second same flavor lepton of opposite charge are removed as Z boson candidates if the reconstructed ee or $\mu\mu$ invariant mass is between 75 and 105 GeV/c^2. If a candidate high-E_T photon [10] is present, the three-body mass is used to remove radiative Z candidates. An inclusive W boson sample is selected from the inclusive lepton sample by requiring $\not\!\!E_T > 20$ GeV and that the lepton be isolated from any jet activity. For the latter we define isolation, I, as the transverse energy in a cone of $\Delta R = 0.4$ centered on the lepton, but excluding the lepton energy, divided by the E_T (P_T) of the electron (muon), and require $I < 0.1$. Furthermore, the event must not be accepted as a dilepton candidate [6].

In order to separate $t\bar{t}$ events in the lepton+jets channel from the large W+jets background, we require that one of the jets be identified as a b jet candidate. Identification of b jets is done either by reconstructing secondary vertices from b-quark decay using the SVX (SVX tagging), or by identifying an additional lepton from a semileptonic b decay (SLT tagging). The SVX and SLT tagging algorithms are described in Ref. [4].

The efficiency for tagging a b quark from a top decay is determined from $t\bar{t}$ Monte Carlo data together with a detailed simulation of the detector, which includes the effects of local track density on the track finding efficiency. The systematic uncertainty due to the tracking efficiency modeling is determined by comparing data and Monte Carlo tracking efficiencies and multiplicity distributions as a function of jet E_T in inclusive electron and muon samples, which are enriched in b decays. The efficiency for tagging at least one b quark in a $t\bar{t}$ event with ≥ 3 jets is found to be $(39\pm3)\%$. Of this 39%, a factor of 67% comes from the fiducial acceptance of the SVX.

The SLT algorithm identifies both muons and electrons with $P_T > 2.0$ GeV/c to $|\eta| = 1.0$. The efficiency of this algorithm, as a function of lepton P_T, is measured with photon conversion and $J/\psi \rightarrow \mu\mu$ data, and applied to Monte Carlo $t\bar{t}$ events. The probability of finding an additional e or μ from a b quark decay in a $t\bar{t}$ event with ≥ 3 jets is $(18 \pm 2)\%$.

In the $t\bar{t}$ signal region of $W+\geq 3$ jets, there are 34 SVX-tagged events containing a total of 42 SVX tags, and 40 SLT-tagged events containing a total of 44 SLT tags. Of these, 11 events are tagged by both the SVX and SLT algorithms.

The acceptance for identifying $t\bar{t}$ events in the lepton+jets mode is calculated from a combination of data and PYTHIA [11] and HERWIG [12] $t\bar{t}$ Monte Carlo samples. We use a top mass of 175 GeV/c^2 [13] when evaluating the acceptance. The total acceptance, including the branching fraction, is calculated as the product of the kinematic (including lepton identification) and geometric acceptances, the trigger efficiency and the tagging efficiency. We measure these efficiencies as described in Ref. [3], and average over the two running periods. For the lepton+jets analysis, the product of the geometric and kinematic acceptance is $(10.4\pm1.0)\%$, and the trigger efficiency is $(90\pm7)\%$. These factors are common between the SVX and SLT analyses. Combining with the respective tagging efficiencies gives a total SVX acceptance of $(3.7\pm0.5)\%$ and a total SLT acceptance of $(1.7\pm0.3)\%$.

The systematic uncertainties on the geometric and kinematic acceptances come from the following: the jet energy scale ($\pm5\%$), modeling of initial state gluon radiation ($\pm2\%$), final state gluon radiation ($\pm5\%$), Monte Carlo dependence and modeling ($\pm5\%$), detector resolution effects ($\pm2\%$) and instantaneous luminosity dependence ($\pm1\%$). The uncertainties on the tagging and trigger efficiencies are dominated by the level of agreement between data and the Monte Carlo predictions.

The most important source of background in the SVX-tagged lepton+jets channel is inclusive W production in association with jets containing b or c quarks, eg. $p\bar{p} \rightarrow Wg$ ($g \rightarrow b\bar{b}$). In addition, there are contributions to the background from mistags (i.e. tags in jets which contain no true displaced vertices), and small contributions from the following processes: non-W(e.g. direct $b\bar{b}$ production), single top production, WW, WZ, and Drell-Yan.

To calculate the background from W+heavy flavor events, we use the HERWIG and VECBOS [14] Monte Carlo programs to predict, as a function of jet multiplicity, the fraction of W+jet events which are $Wb\bar{b}$, $Wc\bar{c}$ and Wc. These fractions, and a tagging efficiency for each type of event, are applied to the number of W+jet events seen in the data to give an expected background from these sources for each jet multiplicity. The details of this method can be found in Ref. [3].

The background from events in the sample that do not contain real W bosons (non-W) is calculated from the data by measuring the number of tags as a function of lepton isolation, I, and $\not{E}_{\mathrm{T}}$. The tagging rate in the low $\not{E}_{\mathrm{T}}$, high-I region, where there are essentially no real W events, is used to predict the contamination in the W signal region of high $\not{E}_{\mathrm{T}}$, low I.

To calculate the background from mistags [3], we assume that the distribution of reconstructed transverse decay length, L_{xy}, from this source is symmetric about zero. Secondary vertices with negative L_{xy} (i.e. those which reconstruct to the opposite side of the primary from the jet direction) come primarily from reconstruction errors in light quark jets. We parametrize the negative L_{xy} distribution measured in generic jet data as a function of jet E_{T}, η, and the number of SVX tracks in the jet. This parametrization is applied to the W+jets data to predict the number of mistags observed.

The single top background is determined by measuring the acceptance for W^* and W-gluon production using the PYTHIA and HERWIG Monte Carlo programs, and using the latest theoretical cross sections [15]. The remaining, relatively small, backgrounds (WW, WZ, $Z \rightarrow \tau\tau$) are derived from Monte Carlo predictions.

The individual components of the background and their totals are shown in Table I. In addition to the signal region of 3 or more jets, we show the predicted number of tags in events with 1 and 2 jets as a check of our calculation. An iterative correction, to account for the $t\bar{t}$ content of the W+jet events, is applied to those backgrounds that are calculated as a fraction of the observed number of these events [3]. The corrected background in the signal region is 9.2$\pm$1.5 tagged events. We observe 34 tagged events, resulting in a cross section of $6.2^{+2.1}_{-1.7}$ pb.

The background to SLT-tagged events is dominated by W events with hadrons misidentified as leptons (including decays in flight), with electrons from unidentified photon conversions, or with real heavy flavor jets ($Wb\bar{b}$, $Wc\bar{c}$). These backgrounds are calculated by measuring the fraction of tags per track in a generic jet sample as a function of the track P_T. These fractions are applied to tracks in the W+jet events to estimate the background from the above sources. Smaller backgrounds are, in order of importance in the signal region, WW and WZ, non-W, $Z \to \tau\tau$, single top, Wc, and Drell-Yan production. The results of the background calculation and the number of tags observed in the data are shown in Table I. In the signal region of $W+ \geq$3 jets, the background prediction is 22.6 $\pm$ 2.8 tagged events. We observe 40 SLT tagged events, resulting in a cross section of 9.2 $^{+4.3}_{-3.6}$ pb.

TABLES

	W+1 Jet	W+2 Jets	W+3 Jets	W+ $\geq$4 Jets
Events before tagging	10 716	1663	254	70
SVX tagged events	70	45	18	16
$Wb\bar{b}+Wc\bar{c}$	19.3 $\pm$6.7	9.7 $\pm$2.4	2.3 $\pm$0.6	0.85 $\pm$0.24
Non-W	7.7 $\pm$3.0	4.0 $\pm$1.5	1.4 $\pm$0.5	0.77 $\pm$0.33
Mistags	20.9 $\pm$6.3	7.2 $\pm$2.1	1.7 $\pm$0.5	0.63 $\pm$0.22
Single top	1.3 $\pm$0.4	2.8 $\pm$0.7	1.0 $\pm$0.4	0.29 $\pm$0.14
Other (incl. Wc)	21.5 $\pm$5.2	7.4 $\pm$1.5	1.3 $\pm$0.2	0.39 $\pm$0.08
Uncorrected bkgnd total	71 $\pm$11	31 $\pm$4	7.7 $\pm$1.1	2.9 $\pm$0.5
Corrected bkgnd total	71 $\pm$11	31 $\pm$4	7.2 $\pm$1.1	2.0 $\pm$0.4
SVX tagged $t\bar{t}$ expected	1.0$\pm$ 0.3	6.9$\pm$2.1	13.3$\pm$3.6	17.7$\pm$4.7
SLT tagged events	241	78	25	15
Mistags+$Wb\bar{b}$+$Wc\bar{c}$	235 $\pm$21	66.6 $\pm$6.1	15.1 $\pm$1.4	6.8 $\pm$0.7
Single top	0.9 $\pm$0.3	1.5 $\pm$0.5	0.6 $\pm$0.3	0.2 $\pm$0.1
Other	33.1 $\pm$10.6	9.6 $\pm$3.0	1.2 $\pm$1.4	0.6 $\pm$0.6
Uncorrected bkgnd total	269$\pm$23	77.7$\pm$6.6	16.9$\pm$2.0	7.6$\pm$0.9
Corrected bkgnd total	269$\pm$23	77.7$\pm$6.6	15.9$\pm$2.0	6.7$\pm$0.8
SLT tagged $t\bar{t}$ expected	0.8$\pm$0.2	3.8$\pm$1.2	6.6$\pm$1.7	7.7 $\pm$2.1

TABLE I. Summary of event yields from the lepton+jets analyses. The expected $t\bar{t}$ contribution is calculated using the measured combined cross section from this paper.

Our best measurement of the $t\bar{t}$ cross section comes from combining the results of the lepton+jets analyses with the dilepton and all-hadronic analyses [6,7]. The results of the individual analyses are summarized in Table II. The dilepton analysis finds 9 candidate events, with an expected background of 2.4±0.5. The all-hadronic analysis has two parallel paths, one which requires a single SVX tagged jet plus kinematic cuts to isolate $t\bar{t}$, and a second which requires two SVX tagged jets, but no additional kinematic cuts. The single tag analysis identifies 187 candidate events with an expected background of 142±12 events, while the double tag analysis identifies 157 candidates and predicts 120±18 background events. There are 34 candidate events in common between the two analyses. The dilepton, lepton+jets, and all-hadronic data samples are exclusive sets.

We calculate the $t\bar{t}$ production cross section from the combined results of the dilepton and lepton+jets channels using the same maximum likelihood technique described in [3]. The all-hadronic result is added by including the multivariate Gaussian term described in Ref. [7]. The likelihood properly accounts for correlated systematic uncertainties, such as the uncertainty on the integrated luminosity, and the uncertainty on the lepton+jets geometric and kinematic acceptance, which is common to both the SVX and SLT analyses.

	Lepton+Jets		Dilepton	All-Hadronic	
Tag	SVX	SLT	not req.	SVX	2 SVX
$\epsilon_{\rm tag}$	0.39±0.03	0.18±0.02	–	0.42±0.04	0.11±0.02
$\epsilon_{geo \cdot kin}$	0.104±0.010		0.0076±0.0008	0.106±0.021	0.263±0.045
$\epsilon_{trigger}$	0.90 ± 0.07		0.98±0.01	$0.998^{+0.002}_{-0.009}$	
$\epsilon_{\rm total}$	0.037±0.005	0.017±0.003	0.0074±0.0008	0.044±0.010	0.030±0.010
Obs. Events	34	40	9	187	157
Background	9.2 ±1.5	22.6 ±2.8	2.4 ±0.5	142 ±12	120 ±18
$\sigma_{t\bar{t}}$ (pb)	$6.2^{+2.1}_{-1.7}$	$9.2\ ^{+4.3}_{-3.6}$	$8.2^{+4.4}_{-3.4}$	$9.6^{+4.4}_{-3.6}$	$11.5^{+7.7}_{-7.0}$

TABLE II. Summary of acceptance factors and measured cross sections for each analysis channel. The acceptances are calculated for a top quark mass of 175 GeV/c^2.

In Figure 1 we show the results of the cross section calculation for each $t\bar{t}$ decay channel, as well as the combined measurement. The combined cross section for $M_{top} = 175$ GeV/c^2 is $7.6^{+1.8}_{-1.5}$ pb , where the quoted uncertainty includes both statistical (± 1.2 pb) and systematic effects. Due to the mass dependence of the acceptances, the calculated cross section changes by $\pm 10\%$ for a ± 15 GeV/c^2 change in top mass from 175 GeV/c^2. Theoretical calculations [1] range from 4.75 pb to 5.5 pb for $M_{top} = 175$ GeV/c^2. From the ratio of the measured cross sections in the dilepton, lepton+jets and all-hadronic channels we can calculate the branching fraction for a top quark decay to a final state electron or muon. Assuming lepton universality and W decay acceptance, the apparent branching fraction to an electron or muon is 0.188+/-0.048, consistent with the standard model expectation of $\frac{2}{9}$. Specifics of possible non-standard model top decays have not yet been considered.

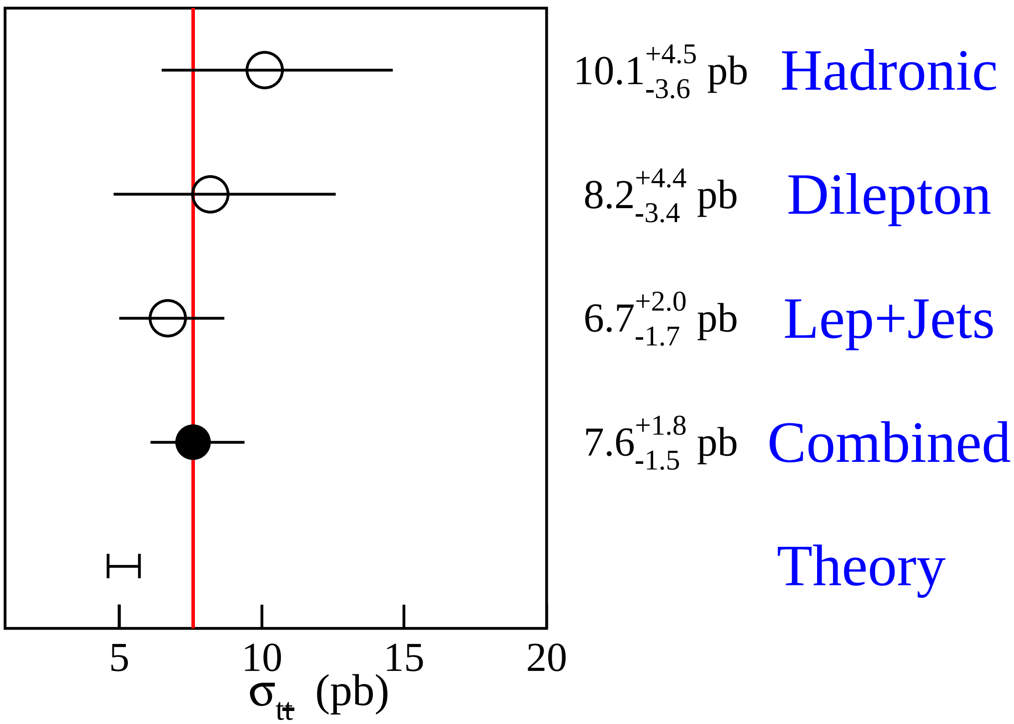

FIG. 1. Measured $t\bar{t}$ production cross section at M_{top}=175 GeV/c^2 for each of the decay channels and for the combined measurement. The lepton+jets cross section is calculated from the SVX and SLT analyses described in the text. The line is drawn through the central value of the combined measurement. The theory point shows the spread in the central values of the 3 most recent predictions [1].

We thank the Fermilab staff and the technical staffs of the participating institutions for their vital contributions. We are grateful for conversations with T. Stelzer and S. Willenbrock. This work is supported by the U.S. Department of Energy and the National Science Foundation; the Natural Sciences and Engineering Research Council of Canada; the Istituto Nazionale di Fisica Nucleare of Italy; the Ministry of Education, Science and Culture of Japan; the National Science Council of the Republic of China; and the A.P. Sloan Foundation.

REFERENCES

[1] E. Berger and H. Contopanagos, Phys. Rev. **D54**, 3085 (1996); S. Catani *et al.*, Phys. Lett. **B378**, 329 (1996); E. Laenen, J. Smith, & W.L. Van Neerven, Phys. Lett. **B321**, 254 (1994); P. Nason, S. Dawson & R.K. Ellis, Nucl. Phys. **B303**, 607 (1988).

[2] K. Lane, Phys. Rev. **D52**, 1546 (1995) and refs. therein; G. Kane, Phys. Rev. Lett. **77**, 3502 (1996).

[3] F. Abe *et al.*, Phys. Rev. **D50**, 2966 (1994); F. Abe *et al.*, Phys. Rev. Lett. **73**, 225 (1994).

[4] F. Abe *et al.*, Phys. Rev. Lett. **74**, 2626 (1995).

[5] S. Abachi *et al.*, Phys. Rev. Lett. **74**, 2632 (1995); S. Abachi *et al.*, Phys. Rev. Lett. **79**,1203 (1997).

[6] F. Abe *et al.*, Fermilab-Pub-97/304-E, submitted to Phys. Rev. Lett.

[7] F. Abe *et al.*, Phys. Rev. Lett. **79**, 1992 (1997).

[8] F. Abe *et al.*, Phys. Rev. Lett. **76**, 3070 (1996). Our luminosity measurement uses a total $p\bar{p}$ cross section of 80 mb.

[9] F. Abe *et al.*, Nucl. Instrum. Methods **271A**, 387 (1988); D. Amidei *et al.*, Nucl. Instrum. Methods **350A**, 73 (1994); P. Azzi *et al.*, Nucl. Instrum. Methods **360A**, 137 (1995).

[10] F. Abe *et al.*, Phys. Rev. Lett. **73**, 2662 (1994).

[11] T. Sjöstrand, Comput. Phys. Commun. **82**, 74 (1994). We use PYTHIA V5.7.

[12] G. Marchesini *et al.*, Comput. Phys. Commun. **67**, 465 (1992). We use HERWIG V5.6.

[13] F. Abe *et al.*, Fermilab-Pub-97/284-E, submitted to Phys. Rev. Lett.

[14] F.A. Berends *et al.*, Nucl. Phys. **B357**, 32 (1991).

[15] T. Stelzer and S. Willenbrock, Phys. Lett. **357B** 125 (1995) ; M. Smith and S. Willenbrock, Phys. Rev. **D54**, 6696 (1996); T. Stelzer, Z. Sullivan and S. Willenbrock, hep-ph/9705398.